Nanoplastic-induced Disruption of DPPC and Palmitic Acid Monolayers: Implications for Membrane Integrity

Shamma Jabeen Proma[a], Biswajit Biswas[a] , Mohamed Yaseen Noor[b], Heather C. Allen[a]*
a. Department of Chemistry & Biochemistry, The Ohio State University, Columbus, Ohio 43210, USA.
b. Department of Materials Science and Engineering, The Ohio State University, Columbus, Ohio 43210, USA.
*** Corresponding author**
allen@chemistry.ohio-state.edu

Keywords: nanoplastics, polystyrene, surfactant films, cell membranes, infrared reflection-absorption spectroscopy, Opt-IR, Brewster angle microscopy

Synopsis: Minimal research exists on the fate of environmental nanoplastics at biophysical interfaces. This study reveals alterations in physiologically relevant bio membrane lipid monolayers in presence of polystyrene nanoplastics.

Abstract: Nanoplastics are generated from the fragmentation of microplastics under various environmental conditions in the atmosphere. These tiny pollutants are widespread and can enter the human body through the air we breathe and the food and water we consume. Understanding how nanoplastics interact with different membrane lipids is paramount to discerning the kind of threat they pose in terms of lung alveolar destabilization, impaired cell communication, cell wall disruption, diminished nutrient delivery, and neurotoxicity. In this research, we examined the interaction of polystyrene nanoplastics with palmitic acid and phosphatidylcholine at the air-aqueous interface to identify individual lipid response. Employing a comprehensive experimental approach that includes infrared-reflection absorption spectroscopy (IRRAS), Langmuir isotherms and Brewster angle microscopy (BAM), we investigated chemical and physical changes of lipid monolayer systems with nanoplastics dispersed within the water solution phase. Increasing concentration of the polystyrene nanoplastics in the solution phase led to enhanced interfacial activity; the nanoplastics were observed to incorporate into the monolayer driven by lipid adsorption/complexation to the nanoplastics. The findings in this research are novel and aid in understanding the physical mechanisms through which nanoplastics may alter and impact biophysical interfaces.

Introduction

The cheap cost of manufacturing, durability, lightweight, and hydrophobicity that makes plastic materials useful for the consumer industry is what lends to their potential for environmental harm. When in the environment, plastic waste degrades slowly over hundreds of years due to its resistance to biotic and abiotic degradation pathways. The fragmented debris exhibit long-range transport owing to atmospheric circulation, convection currents, and local wind patterns. In recent years, the ubiquitous presence of plastic pollution, particularly in the form of micro and nanoplastics, has raised significant concerns due to their potential health impacts.[1-3]

The atmospheric presence of micro sized plastic debris is well documented in different parts of the world and clustered into two major groups (i.e., primary and secondary microplastics) depending on their formation route. Primary microplastics are industrially manufactured at micron sizes intentionally.[4] Secondary microplastics originate from the fragmentation of macroplastic litter through physical abrasion or exposure to UV light.[5-6] Regardless of their formation origin, microplastics end up becoming a part of the atmospheric aerosol burden through physical processes. Evidence suggests that these microplastics then enter human body through inhalation of airborne particles, ingestion through contaminated food and water, and dermal contact, essentially resulting in bioaccumulation in the body.[7] Emerging studies have confirmed the presence of microplastics in different parts of human body such as lung, liver, gut, placenta, feces, and within breast milk.[7] In vitro and in vivo studies have also shown that microplastics induce alteration at different biophysical interfaces and potentially inhibit cell growth, and change cell morphology, leading to cytotoxicity through production of reactive oxygen species (ROS).[8-10]

Microplastics (produced commercially or through environmental degradation) subsequently fragment into submicron or nanosized plastics (i.e. nanoplastics) through mechanical stress, chemical erosion, UV-ageing and can persist in air for indefinite time scales.[8, 11] These nanoplastics can be defined as plastic debris with one or more external dimensions in the 1-100

nm range.[12] Detection and characterization of the nanoplastics remain formidable tasks due to limitations in current analytical techniques but their coexistence with environmental microplastics is evident.[8, 13]

Though limited in number, there have been some studies in recent years that explore the effect of nanoplastics on biological systems, including animal models, and the consequential health impacts.[8, 14] The potential pathways for human exposure to nanoplastics are similar to microplastic exposure, but the resulting effect on human health is much more adverse according to current research.[8, 15] The smaller size and larger surface area-to-volume ratio of nanoplastics make them more conducive to cell membrane transport and enable higher bioaccumulation propensity. In vitro and in silico studies have also confirmed the greater ability of nanoplastics to translocate across cell membranes and animal model studies show proof of neuron death due to nanoplastic breach of the blood-brain-barrier.[14, 16-17] Once internalized, nanoplastics can diffuse across biological barriers, such as the respiratory and gastrointestinal epithelia, and accumulate in vital organs as evident by local inflammation observed in the pulmonary system and gastrointestinal tract due to nanoplastic accrual.[15, 18] As such, these internalization pathways raise concerns about nanoplastic-induced toxicity and potential health impacts, necessitating a deeper molecular-level understanding of their interaction mechanisms with physiologically relevant lipids.

This paper focuses on investigating the interactions between polystyrene nanoplastics and key lipid components found in biological membranes, namely palmitic acid (PA) and 1,2-dipalmitoyl-sn-glycero-3-phosphocholine (DPPC). These lipids are fundamental in maintaining cellular membrane integrity, fluidity, and functionality, making them critical targets for understanding nanoplastic-induced behavior. Palmitic acid constitutes approximately 65% fatty acid in human body and 8–32% of the total fatty acids in serum.[19-20] Additionally, palmitic acid is a minor component in pulmonary surfactant (contains 5–10% neutral lipids), which is vital for maintaining alveolar pressure during breathing.[21] As a result, palmitic acid has been utilized in the

pharmaceutical industry for the synthetic preparation of lung surfactant substitutes for therapeutic purposes.[22-25] On the other hand, phospholipids are essential components of biological membranes, forming the structural foundation of cellular environments. The phospholipid bilayers act as a semi-permeable barrier, separating the cell's interior from the external environment, while playing a crucial role in maintaining membrane integrity, regulating the movement of substances, supporting membrane protein functions, and enabling cell communication and signaling.[26] Among the various phospholipids, phosphatidylcholine (PC) is known to be the most abundant in mammalian cellular membranes, and DPPC, a specialized variant of PC, is predominantly found in pulmonary surfactant.[27-28] About 45 wt% of the total phospholipid pool in the pulmonary surfactant is DPPC, which helps regulate surface tension and prevent lung destabilization or collapse.[26-27] Given the significance, it is essential to study how nanoplastics fundamentally interact with these membrane lipids on a molecular level to better understand their impact on cellular environments and biophysical interfaces. Polystyrene (PS) is chosen as a representative of environmental nanoplastics for this research due to its widespread use in consumer industry and in vivo studies confirming the adverse health impact.[8, 14]

Through a combination of advanced experimental techniques including Langmuir isotherms, Brewster angle microscope (BAM) imaging, and infrared-reflection absorption spectroscopy (IRRAS), this study examines how nanoplastics influence the lipid monolayer structure and organization at the air-aqueous interface. Considering the size-dependent removal of nanoplastics from the air due to diffusion and detection limitations in environmental and biological samples, our studies focused on concentrations ranging from 0.6 mg/L to 5 mg/L to maintain environmental relevance based on existing literature.[8-9, 29-30] By varying nanoplastic concentrations and investigating their effect on the membrane lipids in different aqueous environments, the research elucidates the physical mechanisms through which nanoplastics may alter different biophysical interfaces, providing insights for understanding potential cellular and

physiological impacts. The paper begins by examining the effects of commercially available PS nanoplastics on surfactant monolayers in neat water, establishing the fundamental physical mechanisms of the interactions at play and subsequent property changes. These findings are then correlated with the observation of environmentally aged PS nanoplastic impact on a biophysical interface, using aqueous subphase that mimics real-world conditions for broader biological and environmental relevance.

Experimental Methods

Materials

The 100 nm diameter analytical-grade PS nanospheres (CAS number 9003-53-6, MilliporeSigma) are mono dispersed in water with traces of anionic surfactant SDS (~0.07%) and preserving agent NaN_3 (~0.007%), and as such necessary control studies were done (SI, Figure S1). Additionally, the nanospheres have surface sulphate groups from the initiator in the polymerization reaction and carry a negative surface charge (Technical division, MilliporeSigma). This makes them somewhat of a suitable proxy for real-world nanoplastics that exhibit varied surface functionalities. For further environmental relevance, a portion of the nanospheres was also subjected to UV aging to simulate environmental degradation resulting from sun exposure. Palmitic acid (≥99%, Sigma-Aldrich), Deuterated palmitic acid (98%, Cambridge Isotope Laboratories) and DPPC (>99%, Avanti Polar Lipids) were used as received without further purification (Scheme 1). Each surfactant was dissolved in chloroform (HPLC Grade, Fisher Scientific) at a concentration of ~1 mM. The PS nanosphere-aqueous subphases (Table S1) were prepared by mixing appropriate amounts of PS nanosphere-water dispersion stock with ultrapure water (pH= 5.8,18.2 MΩ·cm resistivity, Milli-Q Advantage A10) or buffer subphases. Powdered phosphate buffered saline i.e.,

PBS (Sigma Aldrich) was dissolved in water to mimic the non-toxic cell environment (10 mM PBS, 138 mM NaCl, 2.7 mM KCl, pH= 7.4).

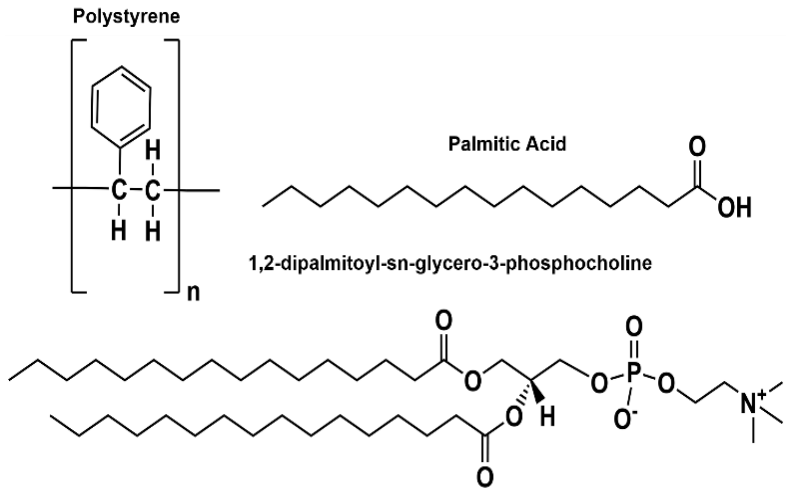

Scheme 1. Molecular structures of the materials used in the study

Methods

UV-Aging of the PS nanospheres. A 340 nm polychromatic UV lamp was used to continuously irradiate the PS nanosphere-water stock solution for one month with an intensity of 8.1 W/m², simulating a theoretical environmental aging equivalent to approximately two months.[31] This approach effectively mimics the emission spectra of the sunlight reaching Earth (95% UV-A and 5% UV-B) as the lamp spans the region of 300–405 nm. The method is a reliable simulation of real-world UV exposure of environmental plastic debris due to solar weathering with appropriate intensity and wavelength selection as discussed in previous research.[31]

Optical Photothermal Infrared (OPT-IR) Spectroscopy. Simultaneous IR and Raman spectra of the PS nanospheres deposited on a ceramic alumina slide (MSE Supplies) were collected using the mIRrage-LS Microscope (Photothermal Spectroscopy Corp) and the experimental details can be found in SI.

Zeta potential. Zeta potential measures the electrical potential at the interface between a solid surface and the surrounding liquid, providing an effective way to quantify the surface charge of nanoparticles.[32] The Brookhaven 90 Plus PALS was used to measure the zeta potential of the PS nanosphere-aqueous solutions following standard procedure.

Atomic Force Microscopy. The morphology of the PS nanospheres was analyzed using Atomic Force Microscopy (AFM) for 3D imaging at the nanoscale using a Bruker AXS Dimension Icon Atomic Force Microscope in ScanAsyst mode following similar procedure in previous research.[33]

Surface Pressure-Area (π-A) Isotherm. Surface pressure (π) is the measured difference in surface tension of a water subphase in absence (γ_0) and presence (γ_m) of a thin film covering the surface i.e., $\pi = (\gamma_0) - (\gamma_m)$. Surface pressure measurements allow for an exploration of intermolecular forces at the interface and give information on the surface organization and structural changes.[34-36] All π-A isotherms were performed using a platinum Wilhelmy plate in the same Teflon Langmuir trough at constant rate of 2.5 mm/min/barrier, the lower mechanical compression rate enabled higher metastability to the isotherms under the experimental non-equilibrium condition, leading to less fluctuation/instrumental artifact during the observation time.[37] Isotherms were recorded at 20 ± 0.6 ºC and a relative humidity of 31 ± 10%, the experimental details can be found in SI.

Brewster Angle Microscopy (BAM). BAM is a microscopic imaging technique used to determine the surface morphology and optical properties of insoluble organic films at the air-aqueous interface. We used a custom-built BAM set up to investigate microstructural changes of the lipid monolayers that exhibits spatial resolution of less than 2 μm and is capable of distinguishing between surfactant aggregates of ~10 μm.[38-40] The detail on the instrumentation can be found in the SI (Scheme S1). The lipid monolayers were spread dropwise on neat water and PS nanosphere-aqueous solutions in acid-cleaned petri dishes (57 mm diameter) to desired mean molecular areas (MMAs) that correspond to distinct phases in the isotherms with different packing

structure. It is important to note that the interface reaches an equilibrium in the drop-casting method used here and effectively provides insights into the fundamental interactions between surfactant molecules and nanoplastics, without the external perturbation and artifacts caused by mechanical compression, which has been shown to alter domain structures in monolayers in previous research.[41-42] The images were reproduced over a timespan of ~2-3 hours to ensure reproducible morphological and shape distributions of the lipid monolayers over time. All data were recorded at 20 ± 0.6 ºC and 31 ±10 % humidity. The BAM images were processed using ImageJ software (version 1.54f) and cropped from their original size to portray only the regions of focus without any further editing.

Infrared Reflection-Absorption Spectroscopy. IRRAS is a surface-sensitive spectroscopic technique used to determine the chemical and physical signature (i.e., surface organization) of surfactant or lipid films on condensed phase surfaces. We used a custom-built optical set up in a Fourier transform infrared spectrometer (Frontier, PerkinElmer) coupled with a liquid-nitrogen-cooled HgCdTe (MCT) detector, more information on the theory of IRRAS and the experimental set up can be found in SI and previous literature.[35, 43-45,] The IRRAS spectra were collected in acid-cleaned petri dishes at the desired mean molecular area as described previously.[40] Throughout the experiments, the surface pressure remained consistent with the distinct phases observed in the respective isotherms of PA and DPPC, with time relaxation studies showing no significant changes (Figure S2). Data analysis was performed using Origin software (OriginPro 9) and the spectra were plotted without any background subtraction or smoothing. The spectra were reproduced at least 3-6 times, and the peaks were evaluated by the data reader function in Origin. Peak shifts to higher or lower wavenumber in nanoplastic presence are only reported if the values fall outside the range of standard deviation of the respective peaks for lipid experiments on neat subphases. Experiments were carried out at 19.1 ± 1.0 °C and a relative humidity of 30 ± 10%.

Results and Discussion

Spectral characterization of the PS nanospheres. The reflection mode IR spectra of the PS nanospheres displayed all the characteristic peaks and matched standard database for the chemical to a great extent as detailed in SI (Figure S3).[9, 46-48] .Concurrently, the Raman spectra also exhibited a substantial agreement with the polystyrene database.

On the other hand, The IR mode spectra of the UV-aged PS nanospheres showed spectral variation at different locations on the slide and overall, some changes were seen from the pristine/commercial version (Figure S4). However, it should be noted that a large portion of the aged nanoplastics also showed identical spectral composition to the pristine version. Due to the solar weathering, some of the PS appeared to have undergone degradation, as the O-C-O stretching at the ~1070 cm^{-1} and the C-OH tensor at the 1372 cm^{-1} did not show up in the spectra. Appearance of additional peaks were also observed, noticeably in the regions of ~1470 and ~1506 cm^{-1}. The peak at the 1506 cm^{-1} region can be attributed to the C-C stretching in an aromatic ring, and interestingly, the peak at ~1470 cm^{-1} is usually seen in acyclic alkane for the asymmetric C-H bending.[49-50] Sujon et al. using the same aging method, reported no such spectral changes in their PS films, reason for which might be the shorter aging time in their experiment.[31] The PS nanosphere-water stock solution also sported an almost unnoticeable pale-yellow tint after aging, that hints at degradation or reduced structural integrity. This might be due to dissociation or scission at the polymer chains as described by Huang et al and is consistent with the appearance of the additional peaks.[51]

Surface charge and morphology analysis of the PS nanospheres. The average zeta potential of the PS nanosphere-aqueous solutions was about -35.13 $\pm$ 0.75 mV, indicating stability of the strongly anionic colloidal dispersion.[32, 52] In contrast, the UV-aged PS nanosphere-aqueous solutions exhibited a zeta potential of approximately -29.27 $\pm$ 3.01 mV. While still highly anionic, the increased fluctuation suggests potential instability, likely due to the agglomeration of

disintegrated plastic debris.[32] The AFM images of the PS nanospheres reveal a consistent height and morphological distribution (Figure S5). Interestingly, UV-aging the pristine PS under solar conditions induced a vastly different morphology. The spheres degraded into structures that seemed flaky or fibrous in nature, with height distribution ranging from 9 to 17 nm.

π-A isotherms of PA in the presence of PS nanospheres in water

To understand the perturbation effect of these nanoplastics on the structure and organization of the lipid monolayers at the fundamental level, we collected π-A compression isotherms of PA monolayers spread on PS nanosphere-aqueous solutions of varying concentrations (Figure 1). The phase behavior of PA on different aqueous solutions is well documented and an isotherm of PA on neat water is also given for reference.[34, 38-39] With decreasing mean molecular area (MMA) at ambient temperature, the PA isotherm exhibits distinct phases (having different packing structures) including the gas-tilted condensed (G-TC) coexistence region, tilted condensed (TC), untilted condensed (UC), and collapse phases. The PA film in our neat water studies underwent a 2D phase transition from G-TC coexistence phase to a TC phase at ~ 22.5 $\pm$ 0.05 Å^2/molecule, known as the lift-off point which shows an increasing surface pressure upon compression of the monolayer. Another phase transition from the TC phase to UC phase is observed at ~18.5$\pm$ 0.06 Å^2/molecule that goes to the collapse at ~17$\pm$ 0.07 Å^2/molecule indicating formation of 3D aggregates from the 2D monolayer (raw and the deviation in MMA for the isotherms can be found in Figures S6 and S7, respectively).

In nanoplastic presence, the PA isotherm during compression moved to both decreased and expanded MMAs, which might be indicative of two different mechanisms involving the lipids and the PS nanospheres. For aqueous solutions with polystyrene concentration below 1 mg/L, the π-A isotherms moved towards the direction of decreasing surface area on average (lift-off point

decreased by ~1.5 Å^2/molecule). The result is similar to what was previously recorded in isotherm studies of animal-derived lung surfactant monolayers in polystyrene microsphere (<1μm diameter) presence of similar concentration.[9] This was described as an indication of the surfactant molecules adsorbing onto the surface of PS nanospheres dispersed in water while being compressed to decreasing surface area. Such behavior is expected to cause surfactant loss from the interface, and although PA is a minor component in natural lung surfactant, we believe similar mechanism might be at play for our studies too.

However, we see a different trend at higher concentrations (4-8 times higher than the initial 0.6 mg/L) in our compression isotherms. With increasing concentration, the isotherms on average move towards increasing surface area (lift-off point increased up to 2 Å^2/molecule). Such surface area expansion of lipid isotherms can be explained by intercalation/aggregation of the PS nanoplastics with the surface-deposited lipid layer.[53] Notably, for the 2.5 mg/L PS nanosphere-aquesous subphases, the isotherms remained closely aligned with those observed for PA films in neat water (Figures S6 and S7).

The nanoplastics used in our studies have a very large surface area-to-volume ratio that leads to increased bioavailability, the PS nanospheres as such might be interacting with the lipid monolayers through different mechanisms such as adsorption/complexation.[22, 54-55] The dispersed nanospheres in Brownian motion can modify the surface composition and structure of the monolayer inducing destabilization at the interface through different non-specific interactions. Consequently, as previously suggested in similar studies, the adsorption of lipid molecules onto the nanosphere surface or the formation of complexes with the nanospheres may dominate, leading to the incorporation of these structures into the lipid monolayer or surfactant loss from the interface.[9, 22, 53-54] The shifted PA isotherms in nanoplastic presence in Figure 1 is consistent with the assumption of such adsorption phenomenon, indicating the existence of interactions between the nanoplastics and the surface lipid molecules.

We also explored the changes in compressibility modulus of the isotherms in nanoplastic presence, details of which can be found in SI (Figure S8). But briefly, the nanoplastics significantly disrupted the characteristic close molecular packing of the UC phase, hinting at an increased fluidity of the monolayers due to weaker lipid-nanoplastic interactions or weakening of the lateral cohesion interactions within the monolayer.[53, 56,]

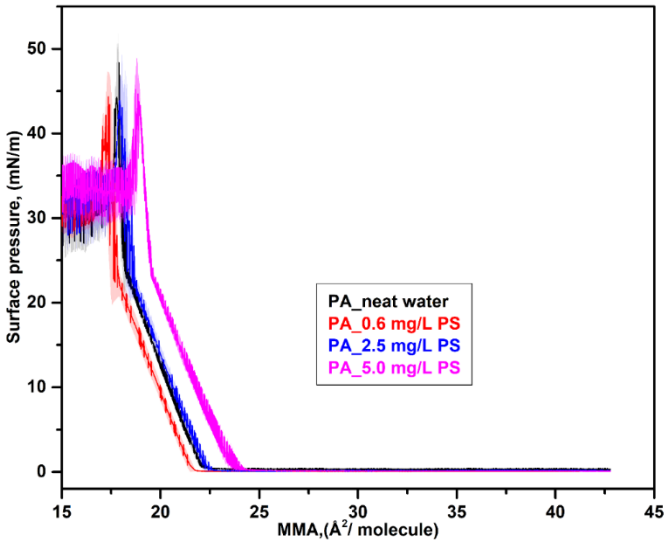

Figure 1. Surface pressure-area isotherms of PA monolayer spread on aqueous solutions of polystyrene nanospheres. *The shaded areas represent standard deviation*.

BAM of PA in the presence of PS nanospheres in water

We used BAM to investigate the microstructure of a PA monolayer spread on aqueous solutions of polystyrene nanospheres to further explore the adsorption/complexation phenomena noted in the isotherm studies. At the G-TC phase (around 35 Å^2/molecule), PA on neat water shows characteristic large, homogenous circular domains that can be described as two-dimensional aggregation of the PA molecules, indicating the coexistence of the 2D gas phase and tilted condensed phase in this region.[38, 57] The bright domains suggest condensed phases with uniform molecular orientation of the surfactant chains whereas the dark regions correspond to the aqueous surface or surfactant-poor regions.[35] Although our isotherm studies show no impact in

this region, it is evident from Figure 2(b-d) that, at the same MMA of 35 Å^2/molecule, with increasing PS concentration in the aqueous solutions, the brightness of the surface decreased significantly, and the lipid surface became more porous compared to neat water (Figure 2a). It is important to note that the polarization angle of the incoming light and exposure time were kept constant across all BAM images, and as such, changes in intensity of the reflected light indicate changing density of the surfactant molecules at the interface with the presence of nanoplastics. Upon addition of nanoplastics to the water subphase, the large circular domains disintegrated into smaller domains and appearances of dark "holes" or porous regions were also observed. These dark regions, along with the altered film structure, are usually attributed to disordered and low lipid-density areas within the monolayer.[35] Therefore, we conclude that some PA molecules are solubilizing and are removed from the surface in nanoplastic presence leading to surfactant loss, as suggested by the PA isotherm shifting to decreased MMA in 0.6 mg/L PS nanosphere-aqueous solutions. These changes in interfacial microstructure and lipid loss strongly indicate the occurrence of adsorption and/or complexation phenomena, as hypothesized in prior sections and supported by previous studies with microplastics and nanoparticles.[9, 53]

We also investigated the changes in the TC phase (~ 20 Å^2/molecule at ~14.6 mN/m) of PA monolayers in nanoplastic presence (Figure S9). For neat water, in the experimental equilibrium-relaxation condition, PA displayed a dense film with dominating presence of floating large 3D aggregates consistent with our findings in a previous study.[58] Interestingly, with nanoplastic presence in the system, the number of such aggregates decreased significantly, which is consistent with surfactant loss phenomena observed in the G-TC phase, and isotherm studies of lower nanoplastic concentration. A probable mechanism for such lipid-plastic interactions and the subsequent loss of surface lipids may involve non-specific interactions between the polar headgroups of the PA molecules and the surface moieties of the PS nanospheres as speculated in previous studies.[22, 53] However, the corresponding region in our raw IRRAS spectra proved too

convoluted to clearly identify a spectral signature for such interactions and we did not carry out any higher order fitting to avoid data treatment of the novel experimental system. Given that the carboxyl headgroup of the PA is undissociated in our experimental condition (pKa of PA= ~8.3-8.9) and the PS nanospheres carry a negative surface charge, we believe it is highly unlikely that electrostatic or coulomb interactions such as attractive forces are driving the adsorption or complexation phenomena. [59-60] As such, we speculate the possibility of physisorption as a mechanism, where the hydrophobic nature of the PS is leading to adhesion or wrapping of lipid molecules around the nanospheres.

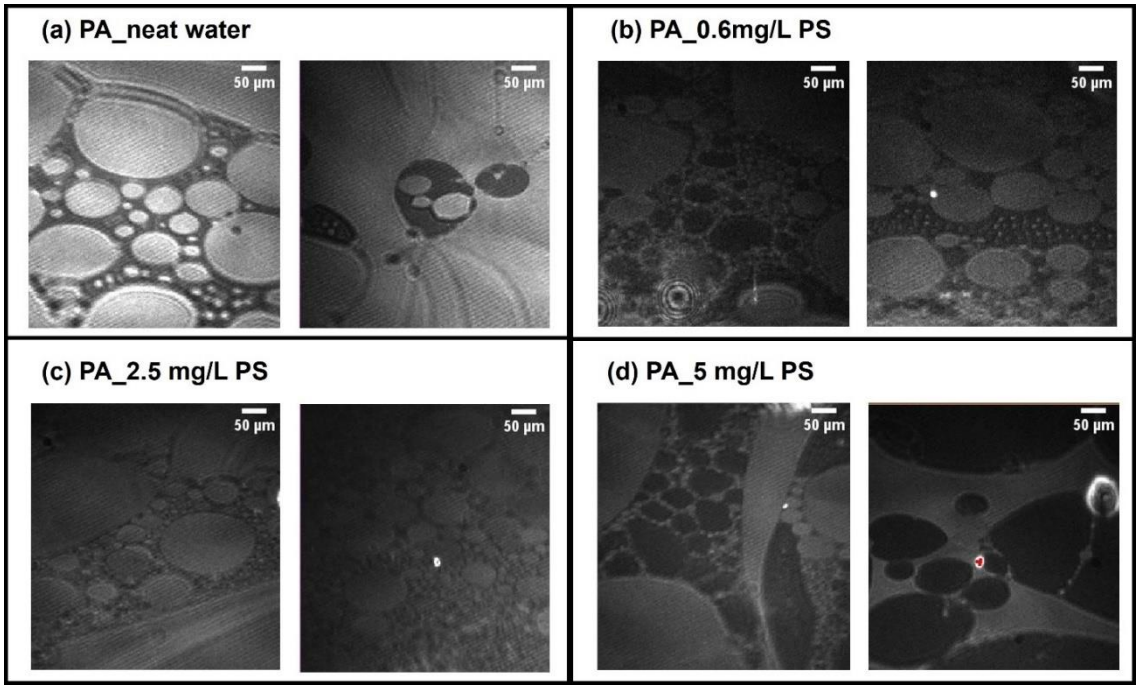

Figure 2. BAM images of PA monolayer in G-TC phase at ~ 35 Å^2/molecule with or without polystyrene nanospheres in the aqueous solution phase at different concentrations. (Red marker in 2(d) is an artifact (SI); all images are cropped into 600 µm x 600 µm snapshots with 50 µm scale bar.)

π-A isotherms of DPPC in the presence of PS nanospheres in water

As phospholipids are one of the most essential components of bio membranes, we next studied the effect of the PS nanospheres on DPPC monolayers. With increasing nanoplastic presence, the DPPC isotherms on average moved towards increasing surface area in the similar concentration range studied (Figure 3). The DPPC isotherm on neat water upon compression exhibited the following phases: gaseous (G), liquid-expanded (LE), LE-liquid-condensed (LC) coexistence plateau region, and LC as typically seen in literature.[41, 61-63] All these phases were also present for DPPC monolayers on PS nanosphere-aqueous solutions and an increase in MMA occurred at both low and high surface pressure regions of the compression isotherms with increasing PS nanosphere concentration. However, for the two lower nanoplastic concentrations, the increase in MMA compared to neat water was minimal, especially in the low surface pressure regime, where the isotherms remained in close proximity to that of water, almost within the experimental error (Figure S10 and S11). In contrast, the isotherms shifted by ~11 $Å^2$/molecule at high surface pressure and by ~8.5 $Å^2$/molecule at low surface pressure regime for the 5 mg/L PS nanosphere-aqueous solutions. The observed shift towards higher MMA at all surface pressures suggests that there are: 1) intercalation of the nanoplastics into the lipid film, 2) formation of DPPC-PS complexes that are incorporated into the monolayer, and/or 3) an electrostatic repulsion between the phosphatidylcholine (PC) polar headgroups that is forcing them apart due to interfacial nanoplastic presence.[63-64] The observed isotherm shift supports the assumption that the PS nanospheres have interfacial presence and the compressibility modulus studies (SI, Figure S12) show subsequent proof of reduced monolayer rigidity, likely due to the weaker lipid-nanoplastic interactions which weakens the lateral cohesion of the monolayer. Increased bioavailability of the polystyrene nanospheres along with their negative surface charge is attributed to such phenomena.[8, 53]

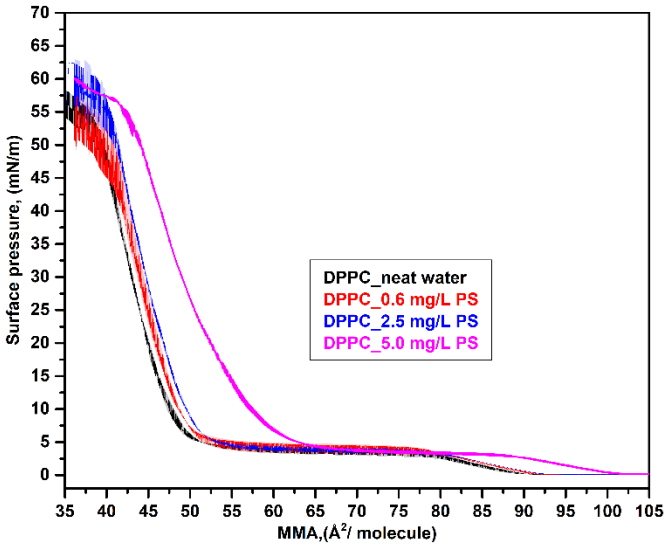

Figure 3. Surface pressure-area isotherms of DPPC monolayer spread on aqueous solutions of polystyrene nanospheres. *The shaded areas represent standard deviation.*

BAM of DPPC in the presence of PS nanospheres in water

Figure 4a illustrates a homogeneous distribution of the small circular domains (~10 µm length) along with 'bean shape' (~20 µm length) formation of DPPC in neat water at the LE-LC region of the monolayer (around 70 Å^2/molecule at ~ 2.07 mN/m) which is regarded as the fundamental shape of DPPC.[42] With PS nanoplastic presence in the subphase, a significant portion of the DPPC domains (at similar MMA), changed in both shape and size with appearance of dark lipid-poor regions that indicates possible surfactant loss from the interface (Figure 4b-d). The bean shape DPPC domains converted to a more elongated, multilobed and/or branched domain structures that were around 140-180 µm in length, creating a heterogenous distribution with the initial bean shapes. Particularly for the 2.5 and 5 mg/L studies, the structures varied between multilobed and branched domains, also described as fractal-like or dendritic shapes in prior literature.[42] It is evident in theoretical calculations and simulation studies that formation of these different shapes is due to the competing effects of line tension and electrostatic dipole-dipole repulsions of the lipid molecules, with the elongated/branched structures being favored by the

repulsion between the polar headgroups.[41, 65-67] As such, the shape and size variation observed might have been a result of different ranges of repulsion in the aggregates. Based on our observation of DPPC isotherms expanding in nanoplastic presence and changes in compressibility modulus, we assert that the nanoplastics are indeed adsorbed at the air-aqueous interface and initiate DPPC expansion through lipid-nanoplastic aggregate formation/complexation.

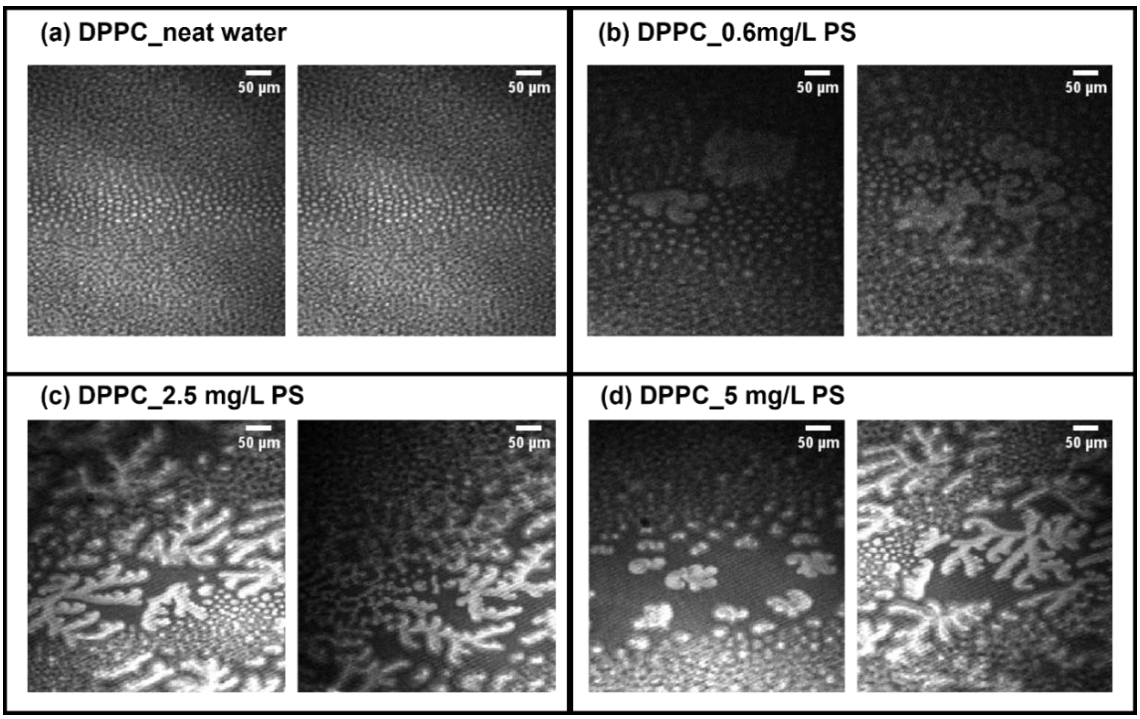

Figure 4. BAM images of a DPPC monolayer in the LE-LC phase~ 70 Å^2/molecule with or without polystyrene nanospheres in the aqueous solution phase at different concentrations. (All images are cropped into 500 µm x 500 µm snapshots with 50 µm scale bar.)

IRRAS of DPPC and PA monolayers in presence of PS nanospheres in neat water

From our π-A isotherm and BAM studies we noted that the PS nanospheres induce structural alterations of PA and DPPC monolayers along with an observed decrease in lipid concentration at the interface or surfactant loss. As such, we carried out surface-sensitive IRRAS experiments

to probe the polar headgroup and methylene stretch region of the DPPC and PA monolayer to identify the chemical signature of the binding/complexation phenomena and the increased disorder among the lipid chains.

Figure 5 depicts IRRAS spectra of the phosphate region for DPPC monolayers on neat water and 5 mg/L PS nanosphere-aqueous solutions at the LE-LC phase (around 58 $Å^2$/molecule at ~2.01 mN/m). DPPC is zwitterionic in aqueous solutions, i.e., carries a positively charged choline moiety and a negatively charged phosphate moiety in its polar head group.[68] For neat water, the symmetric V_S (PO_2^-) and asymmetric V_{As} (PO_2^-) vibrational modes occurred at 1088 cm^{-1} and 1223 cm^{-1}, respectively. With nanoplastic presence in the solution, the asymmetric phosphate stretching on average red shifted to ~1216 cm^{-1} while the symmetric stretching remained unchanged. One contributing factor for this spectral shift might be the inclusion of PS nanospheres at the interface that led to increased repulsion among the PC head groups (i.e., change in electronic environment at the phosphate headgroup) as suggested by the appearance of dendritic/multilobed shaped domains in our BAM studies. This red shift in the phosphate region likely stems from DPPC-PS complex formation, possibly influenced by the charged surface moieties on the polystyrene spheres, similar to the formation of a protein/biomolecular corona facilitated by phospholipid bridging.[9, 62, 69] As previously suggested in case of silica nanoparticles with negative surface charge, the electrostatic interaction between the ammonium group of the DPPC hydrophilic head with the negative charge on the nanosphere surface might be a contributing factor for such complex formation.[53] Yet, the corresponding spectral region proved too convoluted to identify existence of such interaction and as such, we can only speculate as of now.

On the other hand, spectral changes observed at lower nanoplastic concentrations were neither sufficiently pronounced nor reproducible to allow for the identification of definitive interactions or significant changes in the chemical environment at the phosphate headgroup. The lack of clear spectral alterations at these lower concentrations is likely due to a reduced number of interactions

between the PS nanospheres and the DPPC headgroups i.e., insufficient formation of DPPC-PS complexes or surface adsorption, resulting in a lower number density of species that could induce measurable changes in IRRAS (SI). In contrast, the 5 mg/L subphase yielded consistent and reproducible results with spectral shifts that support the hypothesis of DPPC-PS complex formation through electronic environment change at the phosphate region. These findings are further corroborated by BAM observations at this region in nanoplastic presence, which revealed branched domain structures indicative of such complexation for different PS-nanosphere aqueous solutions (Figure S13).

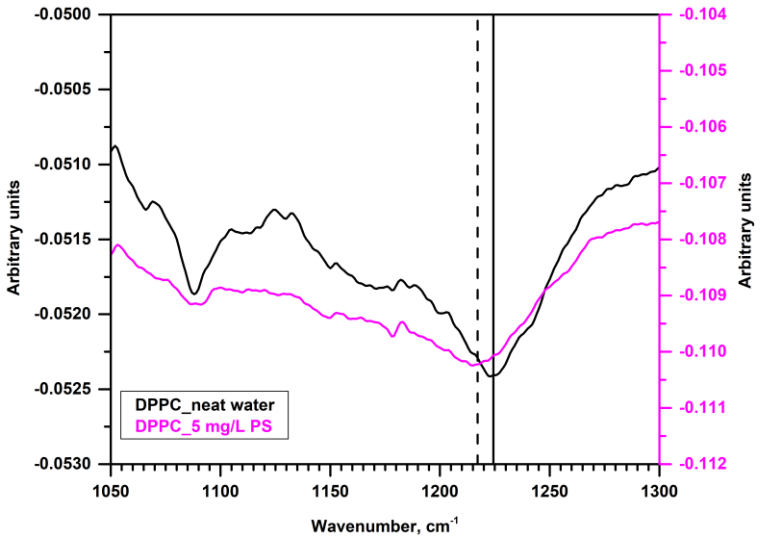

Figure 5. IRRAS spectra of DPPC monolayer spread on neat water and PS nanosphere-aqueous solution in the 1050-1300 cm^{-1} region.

We also investigated the changes in packing structure of PA in the TC phase (~ 20 $Å^2$/molecule at ~14.6 mN/m) due to nanoplastic presence in the solution. In this phase, the hydrophobic carbon tails possess uniform molecular orientation (all trans-extended chains) with the methylene stretching modes at 2800-3000 cm^{-1} region being very sensitive towards external perturbation like interaction of compounds in the subphase with the surface-deposited lipid film.[70] The V_S (CH_2) and V_{As} (CH_2) modes (Figures S14 and S15) found at 2850 cm^{-1} and 2917 cm^{-1} respectively

indicate that the surfactant chains are all-trans extended and nearly perpendicular to the air-aqueous interface for PA spread on neat water in our study.[71] The IR sensitive V_{As} CH_2 mode slightly blue shifted in nanoplastic presence and is an indication of weaker lateral packing among the surfactant chains which aligns well with the nanoplastic-induced disorder of PA molecules observed with BAM and isotherms studies. Despite the very minimal shift, we find it noteworthy to be mentioned, considering the low concentration of nanoplastics in the solution phase ($\geq$ 13.4 pM PS nanospheres).

We additionally studied a deuterated PA monolayer to account for any contribution in the spectral region of methylene vibrational stretch from polystyrene itself and found no such evidence. We also spectrally isolated the CD_2 scissoring mode from the carboxylate region to investigate the packing structure in the chains.[72-74] The $\delta(CD_2)$ was found at 1089 cm^{-1} (Figure S16) for both neat water and nanoplastic solutions of different concentrations and is an indication of hexagonal lattice packing of surfactant chains (a hallmark of long range 2D mesomorphic phase).[75]

Utilizing the above documented experiments, we investigated the interaction of polystyrene nanospheres with PA and DPPC monolayers from a structural and organizational perspective with complementary infrared studies. The compression isotherms and BAM revealed significant alterations in surface behavior and morphology. Observed lipid response in nanoplastic presence aligns well with existing in-vitro studies of microplastic exposure to animal-derived lung surfactants, as both PA and DPPC are components of the pulmonary surfactant mixture, with PA being a minor component and DPPC a major one.[8-9, 21, 27-28] Particularly, our BAM studies shed light on morphological changes with consequential biophysical implications. It's apparent that nanoplastic presence led to lipid loss from the interface that cellular process might not be able adequately compensate for in biological systems, which can result in surfactant inactivity and impaired cell communication.[76] This observation is also consistent with previously published molecular dynamics (MD) simulation studies recording nanoplastics (size 5-10 nm) induced

disruption of the fluidity and ultrastructure of simulated lung surfactant film.[8, 16] Overall, the DPPC monolayers were more affected than PA, with formation of dendritic shaped domains and pores/cavities in the monolayer (i.e., interfacial lipid loss). It is important to note that the number of PA and DPPC molecules in different packing structures at their respective isotherms varied due to their size difference, whereas the number of PS nanospheres in the subphase remained similar. Although the number of DPPC molecules at the surface was always less than PA, we cannot conclusively determine whether this discrepancy contributed to the differing impacts observed. Our IRRAS spectra provided spectroscopic signature of complex formation/interaction between DPPC and PS nanospheres that was suggested in prior in vitro lung surfactant studies, yet spectral validation was previously lacking.

Biophysical relevance: Implications for lung surface

As DPPC is a major component of the lung surfactant, we carried out similar experimental approach with the UV-aged PS nanoplastics in a PBS buffer subphase to mimic the lung environment and evaluate the potential effects of nanoplastic inhalation. Building on the pronounced effects observed in our 5 mg/L fundamental studies with the pristine PS nanospheres, we applied a similar concentration for the aged nanoplastics. Initially, a series of control studies were conducted using aged nanoplastics and a DPPC monolayer in pure water (SI, Figures S17-S19). Interestingly, the qualitative information (i.e., formation of branched domains/pores and red shift at the phosphate region) remained similar to the effects observed with commercial PS nanospheres in our fundamental investigation. Point to be noted is that the 2 months aged nanoplastics still carried similar negative charge and a large portion of them gave identical spectra to the pristine version. As such, our hypothesis of the negatively charged PS nanoplastics interacting with the polar head group through complexation/adsorption remains consistent with the results observed.

As seen in Figure 6 and Figures S20-S21, the DPPC isotherms on PBS subphase expanded to increased MMA compared to neat water, likely due to the screening effect of the counter ions in the PBS subphase.[77] Similar to our previous findings, the DPPC monolayers in PBS subphase expanded to larger areas at low surface pressure region due to incorporation of the UV-aged PS nanoplastics into the lipid monolayer. The transition to LE-LC plateau region was also delayed in nanoplastic presence, which might be a result of the weaker lipid-nanoplastic interactions previously assumed in our neat water studies. These interactions likely resulted in reduced interfacial order and rigidity of the DPPC monolayer, making the film more fluid. During the compression of the condensed phase, the surface pressure increased with a smaller slope in nanoplastic presence and overlapped pure DPPC-PBS isotherm around 13 mN/m. This behavior suggests that some DPPC-PS complexes are squeezed out of the interface under compression, thereby reducing lipid concentration and leading to surfactant inhibition.[53] Consistent with previous findings, the compressibility modulus (Figure S22) also decreased at higher surface pressures in the presence of nanoplastics, further demonstrating a loss of integrity in the surfactant monolayer. [53, 56]

The BAM images of DPPC in the PBS subphase at the LE-LC phase (~70 Å²/molecule) revealed appearance of dark lipid-poor regions with aged nanoplastic presence, in agreement with the interfacial surfactant inhibition predicted by our isotherm studies. There was presence of small multilobed structures, but we did not see the large fractal like shapes, which might have been related to the presence of ions in the PBS subphase interacting with DPPC headgroups. Interestingly, the BAM images of DPPC monolayer with pristine PS nanoplastics in the PBS subphase at the same MMA yielded similar results, i.e., no large, branched domains were seen (Figure S23). As such, we believe that although the solar weathering obviously changed the physical and chemical properties of our nanoplastics, the interaction mechanism remains similar due to the greatly retained chemical characteristics such as similar surface charge and functional

groups. The qualitative results of our investigation align well with findings from previous in-vitro lung surfactant research in the presence of microplastics.[9] As the PBS buffer contains phosphate salts, we refrained from investigating the asymmetric V_{As} (PO_2^-) stretching of DPPC headgroups due to possible convolution effect and the low sensitivity of IRRAS.

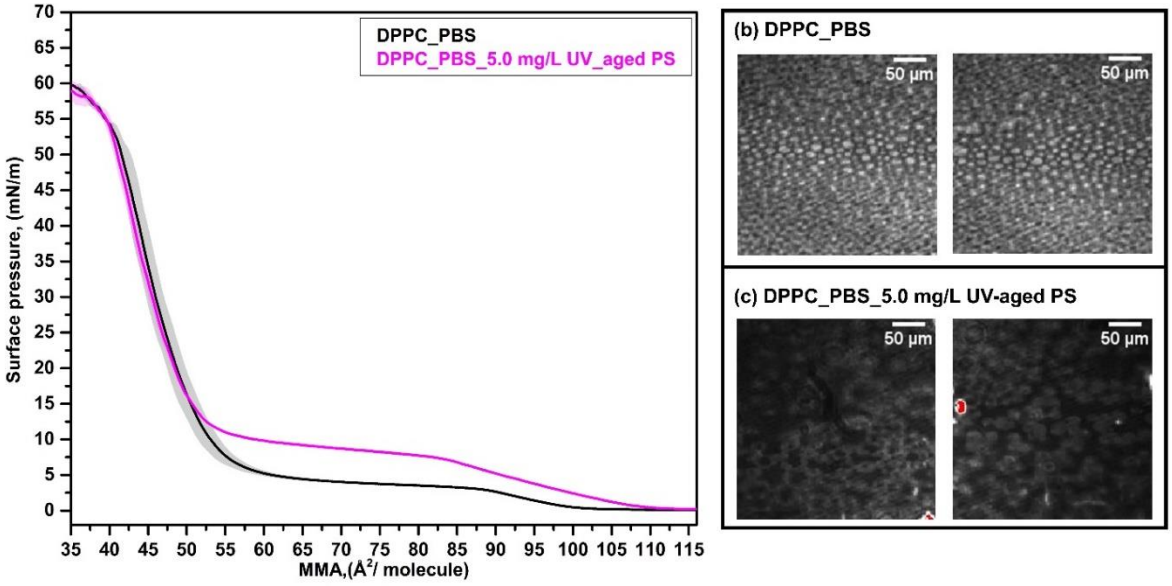

Figure 6. (a) Surface pressure-area isotherms (*The shaded areas represent standard deviation)*; (b) and (c), BAM images of DPPC monolayer (~ 70 Å^2/molecule) with or without UV-aged PS nanoplastics in the 10 mM PBS subphase.(All images are cropped into 300 µm x 300 µm snapshots with 50 µm scale bar.)

While these studies represent a simplified pulmonary surfactant model, the findings provide insights into the underlying interaction mechanisms. Disrupted surfactant monolayers are less effective at reducing surface tension, compromising alveolar stability. The observed lower compressibility modulus and inhibited phase transitions may result in increased breathing effort, mimicking conditions such as respiratory distress syndrome or acute lung injury.[8, 78-81] Similarities between phospholipid monolayers and cell membranes also suggest that the interactions and surfactant loss observed in this study may parallel effects in biological systems exposed to

nanoplastics, impacting crucial processes such as signaling, transport, and membrane protein function.

Associated Content

Supporting information

The supporting information, SI includes additional experimental results and discussion of the methods used.

Author Information

Corresponding Author

Heather C. Allen- Professor, Department of Chemistry & Biochemistry, The Ohio State University, Columbus, Ohio, 43210, United States. Phone: 614-292-4707; Email-allen@chemistry.ohio-state.edu

Authors

Shamma Jabeen Proma- Department of Chemistry & Biochemistry, The Ohio State University, Columbus, Ohio, 43210, United States.

Biswajit Biswas- Department of Chemistry & Biochemistry, The Ohio State University, Columbus, Ohio, 43210, United States.

Mohammed Yaseen Noor- Department of Materials Science and Engineering, The Ohio State University, Columbus, Ohio 43210, USA.

Funding Sources

This research was supported by the Herbert W. Hoover foundation through grant no. GR 130261. The work was also supported by the NSF MRI award CHE-2117225 and the Center for Chemical and Biophysical Dynamics (CCBD) at The Ohio State University.

Acknowledgements

The authors express gratitude to Dr. Sabbir Liakat from Teledyne Princeton Instruments for the invaluable support in rebuilding the Allen Lab BAM set up for this research. We also thank Dr. Eoghan Dillion from Photothermal Spectroscopy Corp, and Dr. Barbara Dunlap, Dr. Yehia Khalifa and Edgar Lopez-Torres from the Department of Chemistry and Biochemistry, Dane Eliott from Environmental Science Graduate Program, The Ohio State University for their assistance in conducting the OPT-IR, AFM and Zeta Potential measurements. We would like to acknowledge Prof. Jahnice Brahney for their idea of aging the nanoplastics for environmental relevance and Shahin Ahmed Sujon, Prof. Kyle Moor for carrying out the aging procedure in their laboratory (Utah State University). We are grateful to Dr. Jessica Clark and Dr. Nicole North (Alumni, Allen Lab) for their guidance and support throughout the project.

References

1. Hernandez, L. M.; Yousefi, N.; Tufenkji, N., Are There Nanoplastics in Your Personal Care Products? *Environ. Sci. Technol. Lett.* **2017,** *4* (7), 280-285. https://doi.org/10.1021/acs.estlett.7b00187
2. Duis, K.; Coors, A., Microplastics in the aquatic and terrestrial environment: sources (with a specific focus on personal care products), fate and effects. *Environ. Sci. Eur.* **2016,** *28* (1), 2. https://doi.org/10.1186/s12302-015-0069-y
3. Sun, Q.; Ren, S.-Y.; Ni, H.-G., Incidence of microplastics in personal care products: An appreciable part of plastic pollution. *Sci. Total Environ.* **2020,** *742*, 140218. https://www.sciencedirect.com/science/article/pii/S0048969720337396
4. Al Harraq, A.; Brahana, P. J.; Arcemont, O.; Zhang, D.; Valsaraj, K. T.; Bharti, B., Effects of Weathering on Microplastic Dispersibility and Pollutant Uptake Capacity. *ACS Environmental Au* **2022,** *2* (6), 549-555. https://doi.org/10.1021/acsenvironau.2c00036
5. Brahney, J.; Mahowald, N.; Prank, M.; Cornwell, G.; Klimont, Z.; Matsui, H.; Prather, K. A., Constraining the atmospheric limb of the plastic cycle. *Proc. Natl. Acad. Sci. U.S.A.* **2021,** *118* (16), e2020719118. https://doi.org/10.1073/pnas.2020719118
6. Allen, S.; Allen, D.; Phoenix, V. R.; Le Roux, G.; Durántez Jiménez, P.; Simonneau, A.; Binet, S.; Galop, D., Atmospheric transport and deposition of microplastics in a remote mountain catchment. *Nat. Geosci.* **2019,** *12* (5), 339-344. https://doi.org/10.1038/s41561-019-0335-5
7. Kutralam-Muniasamy, G.; Shruti, V. C.; Pérez-Guevara, F.; Roy, P. D., Microplastic diagnostics in humans: "The 3Ps" Progress, problems, and prospects. *Sci. Total Environ.* **2023,** *856*, 159164. https://www.sciencedirect.com/science/article/pii/S0048969722062635
8. Xu, X.; Goros, R. A.; Dong, Z.; Meng, X.; Li, G.; Chen, W.; Liu, S.; Ma, J.; Zuo, Y. Y., Microplastics and Nanoplastics Impair the Biophysical Function of Pulmonary Surfactant by Forming Heteroaggregates at the Alveolar–Capillary Interface. *Environ. Sci. Technol.* **2023,** *57* (50), 21050-21060. https://doi.org/10.1021/acs.est.3c06668
9. Shi, W.; Cao, Y.; Chai, X.; Zhao, Q.; Geng, Y.; Liu, D.; Tian, S., Potential health risks of the interaction of microplastics and lung surfactant. *J. Hazard. Mater.* **2022,** *429*, 128109. https://www.sciencedirect.com/science/article/pii/S0304389421030788
10. De-la-Torre, G. E.; Pizarro-Ortega, C. I.; Dioses-Salinas, D. C.; Ammendolia, J.; Okoffo, E. D., Investigating the current status of COVID-19 related plastics and their potential impact on human health. *Curr. Opin. Toxicol.* **2021,** *27*, 47-53. https://www.sciencedirect.com/science/article/pii/S2468202021000371
11. Ivleva, N. P., Chemical Analysis of Microplastics and Nanoplastics: Challenges, Advanced Methods, and Perspectives. *Chem. Rev.* **2021,** *121* (19), 11886-11936. https://doi.org/10.1021/acs.chemrev.1c00178
12. Heddagaard, F. E.; Møller, P., Hazard assessment of small-size plastic particles: is the conceptual framework of particle toxicology useful? *Food Chem. Toxicol* **2020,** *136*, 111106. https://www.sciencedirect.com/science/article/pii/S0278691519308968
13. Gigault, J.; El Hadri, H.; Nguyen, B.; Grassl, B.; Rowenczyk, L.; Tufenkji, N.; Feng, S.; Wiesner, M., Nanoplastics are neither microplastics nor engineered nanoparticles. *Nat. Nanotechnol.* **2021,** *16* (5), 501-507. https://doi.org/10.1038/s41565-021-00886-4
14. Shan, S.; Zhang, Y.; Zhao, H.; Zeng, T.; Zhao, X., Polystyrene nanoplastics penetrate across the blood-brain barrier and induce activation of microglia in the brain of mice. *Chemosphere* **2022,** *298*, 134261. https://www.sciencedirect.com/science/article/pii/S0045653522007548
15. López de las Hazas, M.-C.; Boughanem, H.; Dávalos, A., Untoward Effects of Micro- and Nanoplastics: An Expert Review of Their Biological Impact and Epigenetic Effects. *Adv. Nutr.* **2022,** *13* (4), 1310-1323. https://www.sciencedirect.com/science/article/pii/S2161831322000199

16. Li, L.; Xu, Y.; Li, S.; Zhang, X.; Feng, H.; Dai, Y.; Zhao, J.; Yue, T., Molecular modeling of nanoplastic transformations in alveolar fluid and impacts on the lung surfactant film. *J. Hazard. Mater.* **2022,** *427*, 127872. https://www.sciencedirect.com/science/article/pii/S0304389421028417
17. Kermanizadeh, A.; Balharry, D.; Wallin, H.; Loft, S.; Møller, P., Nanomaterial translocation–the biokinetics, tissue accumulation, toxicity and fate of materials in secondary organs–a review. *Crit. Rev. Toxicol.* **2015,** *45* (10), 837-872. https://doi.org/10.3109/10408444.2015.1058747
18. Grodzicki, W.; Dziendzikowska, K.; Gromadzka-Ostrowska, J.; Kruszewski, M. Nanoplastic Impact on the Gut-Brain Axis: Current Knowledge and Future Directions *Int. J. Mol. Sci.* [Online], 2021.
19. Carta, G.; Murru, E.; Banni, S.; Manca, C., Palmitic Acid: Physiological Role, Metabolism and Nutritional Implications. *Front. Physiol.* **2017,** *8*. https://www.frontiersin.org/journals/physiology/articles/10.3389/fphys.2017.00902
20. Fatima, S.; Hu, X.; Gong, R.-H.; Huang, C.; Chen, M.; Wong, H. L. X.; Bian, Z.; Kwan, H. Y., Palmitic acid is an intracellular signaling molecule involved in disease development. *Cell. Mol. Life Sci.* **2019,** *76* (13), 2547-2557. https://doi.org/10.1007/s00018-019-03092-7
21. Tabor, B.; Ikegami, M.; Yamada, T.; Jobe, A., Rapid Clearance of Surfactant-Associated Palmitic Acid from the Lungs of Developing and Adult Animals. *Pediatric Res.* **1990,** *27* (3), 268-273. https://doi.org/10.1203/00006450-199003000-00013
22. Guzmán, E.; Liggieri, L.; Santini, E.; Ferrari, M.; Ravera, F., Influence of silica nanoparticles on dilational rheology of DPPC–palmitic acid Langmuir monolayers. *Soft Matter* **2012,** *8* (14), 3938-3948. http://dx.doi.org/10.1039/C2SM07097A
23. Ma, G.; Allen, H. C., Real-Time Investigation of Lung Surfactant Respreading with Surface Vibrational Spectroscopy. *Langmuir* **2006,** *22* (26), 11267-11274. https://doi.org/10.1021/la061476k
24. Ma, G.; Allen, H. C., New Insights into Lung Surfactant Monolayers Using Vibrational Sum Frequency Generation Spectroscopy. *Photochem. Photobiol.* **2006,** *82* (6), 1517-1529. https://doi.org/10.1111/j.1751-1097.2006.tb09807.x
25. Staff, F. J. In *Surfaxin (Lucinactant): An intratracheal suspension indicated for the prevention of respiratory distress syndrome in premature infants*, 2012.
26. Chapter 2 - Cell Membranes. In *Medical Cell Biology (Third Edition)*, Goodman, S. R., Ed. Academic Press: San Diego, 2008; pp 27-57.
27. Waite, K. A.; Vance, D. E., Dimethylethanolamine does not prevent liver failure in phosphatidylethanolamine N-methyltransferase-deficient mice fed a choline-deficient diet. *Biochim. Biophys. Acta, Mol. Cell Biol. Lipids* **2004,** *1636* (2), 175-182. https://www.sciencedirect.com/science/article/pii/S1388198104000150
28. Stachowicz-Kuśnierz, A.; Seidler, T.; Rogalska, E.; Korchowiec, J.; Korchowiec, B., Lung surfactant monolayer – A good natural barrier against dibenzo-p-dioxins. *Chemosphere* **2020,** *240*, 124850. https://www.sciencedirect.com/science/article/pii/S0045653519320892
29. Lenz, R.; Enders, K.; Nielsen, T. G., Microplastic exposure studies should be environmentally realistic. *Proc. Natl. Acad. Sci. U.S.A.* **2016,** *113* (29), E4121-E4122. https://doi.org/10.1073/pnas.1606615113
30. Li, Z.; Feng, C.; Wu, Y.; Guo, X., Impacts of nanoplastics on bivalve: Fluorescence tracing of organ accumulation, oxidative stress and damage. *J. Hazard. Mater.* **2020,** *392*, 122418. https://www.sciencedirect.com/science/article/pii/S0304389420304064
31. Sujon, S. A.; Fabiszak, A.; Brahney, J.; Moor, K. J., Wavelength Sensitive Plastic Photodissolution: Elucidating Quantum Yield Trends for Solar Activation Spectra. *Environ. Sci. Technol.* **2024,** *58* (52), 23138-23147. https://doi.org/10.1021/acs.est.4c05660

32. Selvamani, V., Chapter 15 - Stability Studies on Nanomaterials Used in Drugs. In *Characterization and Biology of Nanomaterials for Drug Delivery*, Mohapatra, S. S.; Ranjan, S.; Dasgupta, N.; Mishra, R. K.; Thomas, S., Eds. Elsevier: 2019; pp 425-444.
33. Linville, J. J.; Mason, M. L.; Lopez-Torres, E. U.; Parquette, J. R., Electrostatic assembly of a multicomponent peptide/amphiphile nanotube. *Nanoscale* **2024,** *16* (6), 2894-2903. http://dx.doi.org/10.1039/D3NR03482H
34. Gaines, G. L., Thermodynamic relationships for mixed insoluble monolayers. *J. Colloid Interface Sci.* **1966,** *21* (3), 315-319. https://www.sciencedirect.com/science/article/pii/0095852266900158
35. Vazquez de Vasquez, M. G.; Rogers, M. M.; Carter-Fenk, K. A.; Allen, H. C., Discerning Poly- and Monosaccharide Enrichment Mechanisms: Alginate and Glucuronate Adsorption to a Stearic Acid Sea Surface Microlayer. *ACS Earth Space Chem.* **2022,** *6* (6), 1581-1595. https://doi.org/10.1021/acsearthspacechem.2c00066
36. Dalla Pozza, G.; Deardorff, D.; Subir, M., Emerging environmental contaminants at the air/aqueous and biological soft interfaces. *Environ. Sci.: Adv.* **2022,** *1* (4), 430-437. http://dx.doi.org/10.1039/D2VA00081D
37. Kwok, D. Y.; Tadros, B.; Deol, H.; Vollhardt, D.; Miller, R.; Cabrerizo-Vílchez, M. A.; Neumann, A. W., Axisymmetric Drop Shape Analysis as a Film Balance: Rate Dependence of the Collapse Pressure and Molecular Area at Close Packing of 1-Octadecanol Monolayers. *Langmuir* **1996,** *12* (7), 1851-1859. https://doi.org/10.1021/la950562+
38. Adams, E. M.; Allen, H. C. Palmitic Acid on Salt Subphases and in Mixed Monolayers of Cerebrosides: Application to Atmospheric Aerosol Chemistry *Atmosphere* [Online], 2013, p. 315-336.
39. Castada, H. Z. Brewster Angle Microscopy Study of Model Lung Surfactant Systems at the Air-Water and Air-Physiological Buffer Interfaces. The Ohio State University, 2010.
40. Neal, J. F.; Zhao, W.; Grooms, A. J.; Flood, A. H.; Allen, H. C., Arginine–Phosphate Recognition Enhanced in Phospholipid Monolayers at Aqueous Interfaces. *J. Phys. Chem. C* **2018,** *122* (46), 26362-26371. https://doi.org/10.1021/acs.jpcc.8b03531
41. Klopfer, K. J.; Vanderlick, T. K., Isotherms of Dipalmitoylphosphatidylcholine (DPPC) Monolayers: Features Revealed and Features Obscured. *J. Colloid Interface Sci.* **1996,** *182* (1), 220-229. https://www.sciencedirect.com/science/article/pii/S0021979796904543
42. McConlogue, C. W.; Vanderlick, T. K., A Close Look at Domain Formation in DPPC Monolayers. *Langmuir* **1997,** *13* (26), 7158-7164. https://doi.org/10.1021/la970898e
43. Flach, C. R.; Gericke, A.; Mendelsohn, R., Quantitative Determination of Molecular Chain Tilt Angles in Monolayer Films at the Air/Water Interface: Infrared Reflection/Absorption Spectroscopy of Behenic Acid Methyl Ester. *J. Phys. Chem. B* **1997,** *101* (1), 58-65. https://doi.org/10.1021/jp962288d
44. Du, X.; Miao, W.; Liang, Y., IRRAS Studies on Chain Orientation in the Monolayers of Amino Acid Amphiphiles at the Air−Water Interface Depending on Metal Complex and Hydrogen Bond Formation with the Headgroups. *J. Phys. Chem. B* **2005,** *109* (15), 7428-7434. https://doi.org/10.1021/jp0441700
45. Clark, J. B.; Allen, H. C., Interfacial carbonyl groups of propylene carbonate facilitate the reversible binding of nitrogen dioxide. *Phys. Chem. Chem. Phys.* **2024,** *26* (21), 15733-15741. http://dx.doi.org/10.1039/D4CP01382D
46. Liang, C. Y.; Krimm, S., Infrared spectra of high polymers. VI. Polystyrene. *J. Polym. Sci.* **1958,** *27* (115), 241-254. https://doi.org/10.1002/pol.1958.1202711520
47. Pinchas, S., Infrared Absorption of Aldehydic C--H Group. *Anal. Chem.* **1955,** *27* (1), 2-6. https://doi.org/10.1021/ac60097a002
48. Zolotarev, V. M., Comparison of polystyrene IR spectra obtained by the T, R, ATR, and DR methods. *Opt. Spectrosc.* **2017,** *122* (5), 749-756. https://doi.org/10.1134/S0030400X1705023X

49. Jha, S.; Mehta, S.; Chen, Y.; Ma, L.; Renner, P.; Parkinson, D. Y.; Liang, H., Correction to "Design and Synthesis of Lignin-Based Flexible Supercapacitors". *ACS Sustain. Chem. Eng.* **2020,** *8* (25), 9597-9598. https://doi.org/10.1021/acssuschemeng.0c04171
50. Lin-Vien, D.; Colthup, N. B.; Fateley, W. G.; Grasselli, J. G., CHAPTER 2 - Alkanes. In *The Handbook of Infrared and Raman Characteristic Frequencies of Organic Molecules*, Lin-Vien, D.; Colthup, N. B.; Fateley, W. G.; Grasselli, J. G., Eds. Academic Press: San Diego, 1991; pp 9-28.
51. Huang, Z.; Wang, H., A review on photochemical effects of common plastics and their related applications. *J. Polym. Sci.* **2024,** *62* (6), 969-997. https://doi.org/10.1002/pol.20230322
52. McNeil, S. E., *Characterization of nanoparticles intended for drug delivery*. Humana Press: New York, 2011; Vol. 697.
53. Guzmán, E.; Liggieri, L.; Santini, E.; Ferrari, M.; Ravera, F., Influence of silica nanoparticles on phase behavior and structural properties of DPPC—Palmitic acid Langmuir monolayers. *Colloids Surf. A: Physicochem. Eng. Asp.* **2012,** *413*, 280-287. https://www.sciencedirect.com/science/article/pii/S0927775711007278
54. Santini, E.; Guzmán, E.; Ravera, F.; Ferrari, M.; Liggieri, L., Properties and structure of interfacial layers formed by hydrophilic silica dispersions and palmitic acid. *Phys. Chem. Chem. Phys.* **2012,** *14* (2), 607-615. http://dx.doi.org/10.1039/C1CP22552A
55. Walczak, A. P.; Hendriksen, P. J. M.; Woutersen, R. A.; van der Zande, M.; Undas, A. K.; Helsdingen, R.; van den Berg, H. H. J.; Rietjens, I. M. C. M.; Bouwmeester, H., Bioavailability and biodistribution of differently charged polystyrene nanoparticles upon oral exposure in rats. *J. Nanopart. Res.* **2015,** *17* (5), 231. https://doi.org/10.1007/s11051-015-3029-y
56. Guzmán, E.; Santini, E.; Ferrari, M.; Liggieri, L.; Ravera, F. Interaction of Particles with Langmuir Monolayers of 1,2-Dipalmitoyl-Sn-Glycero-3-Phosphocholine: A Matter of Chemistry? *Coatings* [Online], 2020.
57. Bringezu, F.; Ding, J.; Brezesinski, G.; Zasadzinski, J. A., Changes in Model Lung Surfactant Monolayers Induced by Palmitic Acid. *Langmuir* **2001,** *17* (15), 4641-4648. https://doi.org/10.1021/la0103158
58. Wellen Rudd, B. A.; Vidalis, A. S.; Allen, H. C., Thermodynamic versus non-equilibrium stability of palmitic acid monolayers in calcium-enriched sea spray aerosol proxy systems. *Phys. Chem. Chem. Phys.* **2018,** *20* (24), 16320-16332. http://dx.doi.org/10.1039/C8CP01188E
59. Kanicky, J. R.; Poniatowski, A. F.; Mehta, N. R.; Shah, D. O., Cooperativity among Molecules at Interfaces in Relation to Various Technological Processes: Effect of Chain Length on the pKa of Fatty Acid Salt Solutions. *Langmuir* **2000,** *16* (1), 172-177. https://doi.org/10.1021/la990719o
60. Vysotsky, Y. B.; Kartashynska, E. S.; Vollhardt, D.; Fainerman, V. B., Surface pKa of Saturated Carboxylic Acids at the Air/Water Interface: A Quantum Chemical Approach. *J. Phys. Chem. C* **2020,** *124* (25), 13809-13818. https://doi.org/10.1021/acs.jpcc.0c03785
61. Adams, E. M.; Casper, C. B.; Allen, H. C., Effect of cation enrichment on dipalmitoylphosphatidylcholine (DPPC) monolayers at the air-water interface. *J. Colloid Interface Sci.* **2016,** *478*, 353-364. https://www.sciencedirect.com/science/article/pii/S0021979716303757
62. Adams, E. M.; Verreault, D.; Jayarathne, T.; Cochran, R. E.; Stone, E. A.; Allen, H. C., Surface organization of a DPPC monolayer on concentrated SrCl2 and ZnCl2 solutions. *Phys. Chem. Chem. Phys.* **2016,** *18* (47), 32345-32357. http://dx.doi.org/10.1039/C6CP06887A
63. Guzmán, E.; Liggieri, L.; Santini, E.; Ferrari, M.; Ravera, F., DPPC–DOPC Langmuir monolayers modified by hydrophilic silica nanoparticles: Phase behaviour, structure and rheology. *Colloids Surf. A: Physicochem. Eng. Asp.* **2012,** *413*, 174-183. https://www.sciencedirect.com/science/article/pii/S0927775711008120

64. Guzmán, E.; Liggieri, L.; Santini, E.; Ferrari, M.; Ravera, F., Effect of Hydrophilic and Hydrophobic Nanoparticles on the Surface Pressure Response of DPPC Monolayers. *J. Phys. Chem. C* **2011,** *115* (44), 21715-21722. https://doi.org/10.1021/jp207713x
65. Barakat, J. M.; Squires, T. M., Shape morphology of dipolar domains in planar and spherical monolayers. *J. Chem. Phys.* **2020,** *152* (23), 234701. https://doi.org/10.1063/5.0009667
66. McConnell, H. M.; Moy, V. T., Shapes of finite two-dimensional lipid domains. *J. Phys. Chem.* **1988,** *92* (15), 4520-4525. https://doi.org/10.1021/j100326a053
67. Keller, D. J.; Korb, J. P.; McConnell, H. M., Theory of shape transitions in two-dimensional phospholipid domains. *J. Phys. Chem.* **1987,** *91* (25), 6417-6422. https://doi.org/10.1021/j100309a021
68. Gorwyn, D.; Barnes, G. T., Interactions of large ions with phospholipid monolayers. *Langmuir* **1990,** *6* (1), 222-230. https://doi.org/10.1021/la00091a036
69. Gardner, L.; Warrington, J.; Rogan, J.; Rothwell, D. G.; Brady, G.; Dive, C.; Kostarelos, K.; Hadjidemetriou, M., The biomolecule corona of lipid nanoparticles contains circulating cell-free DNA. *Nanoscale Horiz.* **2020,** *5* (11), 1476-1486. http://dx.doi.org/10.1039/D0NH00333F
70. Garidel, P.; Fölting, B.; Schaller, I.; Kerth, A., The microstructure of the stratum corneum lipid barrier: Mid-infrared spectroscopic studies of hydrated ceramide:palmitic acid:cholesterol model systems. *Biophys. Chem.* **2010,** *150* (1), 144-156. https://www.sciencedirect.com/science/article/pii/S0301462210000670
71. Cheng, S.; Du, L.; George, C., Understanding the Interfacial Behavior of Typical Perfluorocarboxylic Acids at Surfactant-Coated Aqueous Interfaces. *J. Geophys. Res. Atmos.* **2020,** *125* (13), e2019JD032182. https://doi.org/10.1029/2019JD032182
72. Carter-Fenk, K. A.; Dommer, A. C.; Fiamingo, M. E.; Kim, J.; Amaro, R. E.; Allen, H. C., Calcium bridging drives polysaccharide co-adsorption to a proxy sea surface microlayer. *Phys. Chem. Chem. Phys.* **2021,** *23* (30), 16401-16416. http://dx.doi.org/10.1039/D1CP01407B
73. Vazquez de Vasquez, M. G.; Carter-Fenk, K. A.; McCaslin, L. M.; Beasley, E. E.; Clark, J. B.; Allen, H. C., Hydration and Hydrogen Bond Order of Octadecanoic Acid and Octadecanol Films on Water at 21 and 1 °C. *J. Chem. Phys. A* **2021,** *125* (46), 10065-10078. https://doi.org/10.1021/acs.jpca.1c06101
74. Vazquez de Vasquez, M. G.; Wellen Rudd, B. A.; Baer, M. D.; Beasley, E. E.; Allen, H. C., Role of Hydration in Magnesium versus Calcium Ion Pairing with Carboxylate: Solution and the Aqueous Interface. *J. phys. Chem. B* **2021,** *125* (40), 11308-11319. https://doi.org/10.1021/acs.jpcb.1c06108
75. Rajak, P.; Nath, L.; Bhuyan, B., Liquid Crystals: An Approach in Drug Delivery. *Indian J. Pharm. Sci.* **2019,** *81* (1).
76. Fyfe, J.; Casari, I.; Manfredi, M.; Falasca, M., Role of lipid signalling in extracellular vesicles-mediated cell-to-cell communication. *Cytokine Growth Factor Rev.* **2023,** *73*, 20-26. https://www.sciencedirect.com/science/article/pii/S1359610123000539
77. Tang, C. Y.; Huang, Z.; Allen, H. C., Binding of Mg2+ and Ca2+ to Palmitic Acid and Deprotonation of the COOH Headgroup Studied by Vibrational Sum Frequency Generation Spectroscopy. *J. Phys. Chem. B* **2010,** *114* (51), 17068-17076. https://doi.org/10.1021/jp105472e
78. Zuo, Y. Y.; Veldhuizen, R. A. W.; Neumann, A. W.; Petersen, N. O.; Possmayer, F., Current perspectives in pulmonary surfactant — Inhibition, enhancement and evaluation. *Biochim. Biophys. Acta - Biomembr.* **2008,** *1778* (10), 1947-1977. https://www.sciencedirect.com/science/article/pii/S0005273608001235
79. Chakraborty, A.; Hertel, A.; Ditmars, H.; Dhar, P. Impact of Engineered Carbon Nanodiamonds on the Collapse Mechanism of Model Lung Surfactant Monolayers at the Air-Water Interface *Molecules* [Online], 2020.

80. Liekkinen, J.; de Santos Moreno, B.; Paananen, R. O.; Vattulainen, I.; Monticelli, L.; Bernardino de la Serna, J.; Javanainen, M., Understanding the Functional Properties of Lipid Heterogeneity in Pulmonary Surfactant Monolayers at the Atomistic Level. *Front. Cell Dev. Biol.* **2020,** *8*. https://www.frontiersin.org/journals/cell-and-developmental-biology/articles/10.3389/fcell.2020.581016
81. Bykov, A. G.; Panaeva, M. A., Dynamic Properties of Pulmonary Lipid Monolayers on the Surfaces of Sodium Polystyrene Sulfonate and Polydiallyldimethylammonium Chloride Solutions. *Colloid J.* **2023,** *85* (5), 678-686. https://doi.org/10.1134/S1061933X23600677